CatSper channels are regulated by protein kinase A

Received for publication, December 19, 2017, and in revised form, September 5, 2018 Published, Papers in Press, September 13, 2018, DOI 10.1074/jbc.RA117.001566

Gerardo Orta[‡], José Luis de la Vega-Beltran[‡], David Martín-Hidalgo[§], Celia M. Santi[¶‖], Pablo E. Visconti[§1], and Alberto Darszon[‡2]

From the [‡]Departamento de Genética del Desarrollo y Fisiología Molecular, Instituto de Biotecnología, Universidad Nacional Autónoma de México, Morelos 62250, México, [§]Department of Veterinary and Animal Science, Integrated Sciences Building, University of Massachusetts, Amherst, Massachusetts 01003, and [¶]Department of Obstetrics and Gynecology and [‖]Department of Neurosciences, Washington University School of Medicine, St. Louis, Missouri 63110

Edited by Phyllis I. Hanson

Mammalian sperm must undergo capacitation as a preparation for entering into hyperactivated motility, undergoing the acrosome reaction, and acquiring fertilizing ability. One of the initial capacitation events occurs when sperm encounter an elevated HCO_3^- concentration. This anion activates the atypical adenylyl cyclase Adcy10, increases intracellular cAMP, and stimulates protein kinase A (PKA). Moreover, an increase in intracellular Ca^{2+} concentration ($[Ca^{2+}]_i$) is essential for sperm capacitation. Although a cross-talk between cAMP-dependent pathways and Ca^{2+} clearly plays an essential role in sperm capacitation, the connection between these signaling events is incompletely understood. Here, using three different approaches, we found that CatSper, the main sperm Ca^{2+} channel characterized to date, is up-regulated by a cAMP-dependent activation of PKA in mouse sperm. First, HCO_3^- and the PKA-activating permeable compound 8-Br-cAMP induced an increase in $[Ca^{2+}]_i$, which was blocked by the PKA peptide inhibitor PKI, and H89, another PKA inhibitor, also abrogated the 8-Br-cAMP response. Second, HCO_3^- increased the membrane depolarization induced upon divalent cation removal by promoting influx of monovalent cations through CatSper channels, which was inhibited by PKI, H89, and the CatSper blocker HC-056456. Third, electrophysiological patch clamp, whole-cell recordings revealed that CatSper activity is up-regulated by HCO_3^- and by direct cAMP injection through the patch-clamp pipette. The activation by HCO_3^- and cAMP was also blocked by PKI, H89, Rp-cAMPS, and HC-056456, and electrophysiological recordings in sperm from CatSper-KO mice confirmed CatSper's role in these activation modes. Our results strongly suggest that PKA-dependent phosphorylation regulates $[Ca^{2+}]_i$ homeostasis by activating CatSper channel complexes.

This study was supported by Eunice Kennedy Shriver NICHD, National Institutes of Health Grant RO1 HD38082 (to P. E. V), by Consejo Nacional de Ciencia y Tecnología Grants Fronteras 71 39908-Q and CB 2015/255914 from Mexico (CONACyT) (to A. D.), and by Dirección General de Asuntos del Personal Académico of the Universidad Nacional Autónoma de México (DGAPA-UNAM) Grants IN205516 (to A. D.). The authors declare that they have no conflicts of interest with the contents of this article. The content is solely the responsibility of the authors and does not necessarily represent the official views of the National Institutes of Health.

This article contains Figs. S1 and S2 .

[1] To whom correspondence may be addressed. E-mail: pvisconti@vasci.umass.edu.

[2] To whom correspondence may be addressed. E-mail: darszon@ibt.unam.mx.

Chang and Austin (1, 2) demonstrated independently that sperm must undergo capacitation in the female reproductive tract before being capable of penetrating and fertilizing the egg. During this process sperm undergo numerous physiological, biophysical, and biochemical changes. One of the first responses that occur during sperm capacitation is an increase in intracellular cAMP levels induced by the influx of bicarbonate that activates the atypical soluble adenylyl cyclase Adcy10 (also known as sAC)[3] (3, 4), eventually leading to PKA-dependent signaling events that include an increase in protein tyrosine phosphorylation (5). The key role cAMP plays in capacitation and fertilization has been demonstrated using pharmacological (6) tools for gain and loss of function of cAMP-dependent pathways. The role of cAMP was confirmed using mice lacking either Adcy10 (7, 8) or the sperm-specific splicing variant of the PKA catalytic subunit Cα2 (9). Both these mice are sterile and their sperm cannot fertilize *in vivo* or *in vitro*. Furthermore, Jansen *et al.* (10) demonstrated that sperm from Adcy10 null mice expressing a photoactivated adenylyl cyclase recovered their motility and fertilizing capacity when light-stimulated.

In addition to cAMP, sperm capacitation is also associated with the modulation of $[Ca^{2+}]_i$, and multiple data indicate that Ca^{2+} plays a biphasic role in the regulation of cAMP homeostasis. First, Ca^{2+} positively modulates Adcy10 activity by decreasing this enzyme's K_m toward ATP (11). Second, Ca^{2+} negatively regulates cAMP-dependent pathways activating cAMP degradation by phosphodiesterase 1 (PDE1) and by activating the Ser/Thr phosphatase PPP3C (also known as calcineurin) and therefore stimulating the hydrolysis of Ser/Thr phosphorylation sites downstream of PKA (11).

Work by different groups (12–16) indicates that sperm incubated in media with low extracellular Ca^{2+} concentrations ($<$100 nM) do not undergo hyperactive motility. On the other hand, it has been shown that increasing the concentration of intracellular Ca^{2+} ($[Ca^{2+}]_i$) using Ca^{2+} ionophores such as A23187 resulted in complete loss of motility. However, A23187-treated sperm are not dead; if the ionophore is washed out, they recover motility and undergo hyperactivation (17). More interesting, sperm treated with A23187 as described above can overcome the inhibition of hyperactivation and fer-

[3] The abbreviations used are: sAC, soluble adenylyl cyclase (Adcy10); Em, membrane potential; HC, HC-056456; Em_D, Em + compound; Em_R, Em resting.

tilization produced by blocking cAMP signaling with H89 (17). Altogether, these experiments suggest that, in sperm, Ca^{2+} plays a role downstream of the activation of cAMP-dependent pathways. Despite these findings, how cAMP regulates $[Ca^{2+}]_i$ is not clear.

During capacitation, $[Ca^{2+}]_i$ increases and it has been shown that the sperm-specific Ca^{2+} channel CatSper contributes to the influx of this cation. This channel complex is modulated by changes in intracellular pH (pH_i) and in membrane potential (Em). Mice lacking the CatSper channel complex are sterile and their sperm are unable to undergo the capacitation-associated changes in the sperm motility pattern known as hyperactivation (14, 18–20). CatSper is constituted by a complex that contains nine proteins: four that form a pore through which Ca^{2+} can enter (CatSper 1–4), and five accessory proteins whose roles in hyperactivated motility are less clear (21). The localization of CatSper in the mouse sperm flagella is notable; it is found in four parallel tracks which generate unique Ca^{2+} signaling domains along the principal piece of the flagella.

Although the roles of cAMP and CatSper in sperm capacitation are well established, the extent to which CatSper is modulated by a cAMP-dependent pathway is still controversial. On the one hand, it is well established that permeable cAMP agonists can induce an increase in $[Ca^{2+}]_i$ in sperm (22) and that this stimulatory effect is abolished in sperm from CatSper null mice (18). On the other hand, CatSper does not have any predicted cAMP-binding domain, and recent work by Strünker and co-workers presented evidence that the stimulation of human CatSper by these modified cAMP agonists is because of the chemical moieties modifying the cAMP molecule acting externally on CatSper (22, 23).

To further evaluate this controversy, in the present work we used a combination of experimental strategies. First we showed that HCO_3^- and 8-Br-cAMP induced an increase in $[Ca^{2+}]_i$ in single cells. Both responses were blocked in the presence of the PKA antagonist PKI, as were the responses of 8-Br-cAMP with H89. Second, we used indirect recording of Em changes produced by chelating divalent cations with EGTA to measure CatSper activity (24). Using this methodology we showed that HCO_3^- stimulated CatSper and that this increased activity was blocked by the PKA inhibitors PKI and H89. Finally, the Em data were confirmed using whole-cell patch clamp ionic current recordings. Our results are consistent with a role of PKA in CatSper channel complex regulation. Notably, cAMP in the pipette solution, in whole-cell patch clamp recordings, strongly activates CatSper current and this effect is blocked by the PKA inhibitor PKI and H89. CatSper current was also stimulated by an alkalinization induced by NH_4Cl, but this response was not sensitive, neither to PKI nor Rp-cAMPS, another specific PKA inhibitor. Consistent with these findings, HCO_3^- was unable to stimulate ionic currents in sperm from CatSper KO mice. Altogether our results strongly suggest that CatSper channels are activated by PKA by either direct or indirect phosphorylation, highlighting a connection between these two major signaling pathways required for sperm capacitation.

Results

Bicarbonate increases $[Ca^{2+}]_i$ and this response is inhibited by PKI, a PKA inhibitor

Capacitation involves cAMP production and Ca^{2+} uptake. Because Adcy10 is regulated by HCO_3^- and permeable cyclic nucleotides have been shown to induce $[Ca^{2+}]_i$ increases in mouse sperm, we reexamined the $[Ca^{2+}]_i$ responses to these compounds. Addition of control vehicle in sperm loaded with the Ca^{2+}-sensitive dye Fluo-3 did not elicit any Ca^{2+} responses (Fig. 1*A*). In contrast, addition of HCO_3^- induced a reproducible increase in $[Ca^{2+}]_i$ (Fig. 1*B*). The effect of HCO_3^- upon sperm $[Ca^{2+}]_i$ can be explained by either an HCO_3^--induced stimulation of cAMP synthesis by Adcy10 (3, 4) or by an HCO_3^--dependent intracellular alkalinization with the consequent direct effect on CatSper activity, or furthermore by a combination of both pathways. Consistent with the first possibility, the HCO_3^--induced increase in $[Ca^{2+}]_i$ was blocked by the myristoylated PKA peptide inhibitor PKI (Fig. 1*C*). Furthermore, in agreement with a role of a cAMP-dependent pathway, addition of 8-Br-cAMP (1 mM) induced an increase in $[Ca^{2+}]_i$ (Fig. 1*D*). Moreover, the effect of 8-Br-cAMP was also blocked by the PKA inhibitory peptide PKI (Fig. 1*E*). Average fluorescent traces and average maximal responses are summarized in Fig. 1, *F* and *H* and *G* and *I*, respectively. Although, as described previously (18, 19, 22), permeable cGMP also induces $[Ca^{2+}]_i$ increases (Fig. 2*A*), this response was not blocked by PKI (Fig. 2*B*), suggesting that only the effect of the cAMP analogue is mediated by PKA. Average traces and average maximum responses are summarized in Fig. 2, *E* and *G*, respectively. Regarding changes in pH_i, it is well established that pH_i alkalinization can induce an increase in $[Ca^{2+}]_i$. Consistently, addition of NH_4Cl to sperm elicited an elevation in $[Ca^{2+}]_i$ (Fig. 2*C*); however, contrary to the HCO_3^- effect on $[Ca^{2+}]_i$, the NH_4Cl-induced increase was not blocked by PKI (Fig. 2*D*). These findings are summarized in Fig. 2, *F* and *H*.

The 8-Br-cAMP induced $[Ca^{2+}]_i$ increase is also blocked by H89, another PKA inhibitor

Considering that some undesired effects of PKI have been described (26) and to confirm the involvement of PKA, we tested another PKA inhibitor, H89, which is a ATP-binding site competitive inhibitor. As shown in Fig. S1, the increase in $[Ca^{2+}]_i$ caused by adding 1 mM 8-Br-cAMP (Fig. S1*A*) was prevented by 10 μM of H89 (Fig. S1*B*). Average fluorescent traces and average maximal responses are summarized Fig. S1, *E* and *G*, respectively. These findings agree with the hypothesis that PKA is involved in the cAMP-induced increases in $[Ca^{2+}]_i$ in mouse sperm. The $[Ca^{2+}]_i$ increase induced by 10 mM NH_4Cl (Fig. S1*C*) was also inhibited by 10 μM H89 (Fig. S1*D*). These observations are summarized in Fig. S1, *F* and *H*, respectively.

Bicarbonate stimulates the EGTA-induced mouse sperm Em depolarization in a PKA-dependent manner

Previously we have shown that addition of EGTA to spermatozoa elicited a Na^+-dependent depolarizing response (24, 27). Considering that in the absence of external divalent cations, CatSper has high permeability for Na^+, we hypothesized that

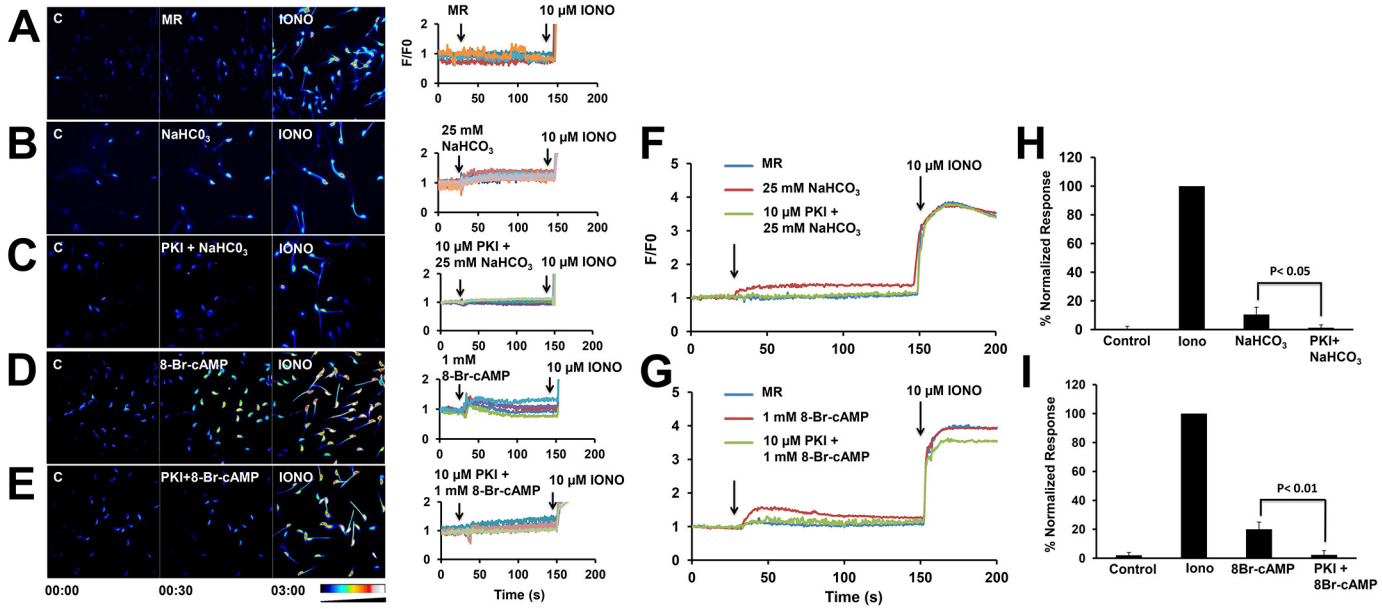

Figure 1. Bicarbonate and 8-Br-cAMP induce a PKA-dependent $[Ca^{2+}]_i$ rise in mouse sperm. *A–E*, representative fluorescence images from Fluo-3 loaded mouse sperm before additions (*c*, control in *A–E*), after adding media (*MR*, negative control in *A*), and in response to 10 μM ionomycin (*IONO*, positive control in *A–E*). *Right panels* show four to five representative single cell fluorescence traces under the different experimental conditions described in the *left middle panels*. *B*, addition of 25 mM $NaHCO_3$ increases $[Ca^{2+}]_i$. *C*, PKI (10 μM) inhibits the $NaHCO_3$ response. *D*, 8-Br-cAMP (cell-permeant cAMP, 1 mM) also elevates $[Ca^{2+}]_i$. *E*, PKI (10 μM) inhibits the 8-Br-cAMP (1 mM) response. Panel *D* is also included in Fig. S1*A*. *F*, average fluorescence traces from sperm (~150 cells) from four different mice subjected to the experimental conditions as in *A–C*. *G*, average traces from four different mice under the experimental conditions shown in *A*, *D*, and *E*. *H*, summary plot of normalized $[Ca^{2+}]_i$ increases maximum responses shown in *F*. *I*, summary plot of normalized $[Ca^{2+}]_i$ maximum increases obtained in *G*. The qualitative color scale indicates low to high $[Ca^{2+}]_i$.

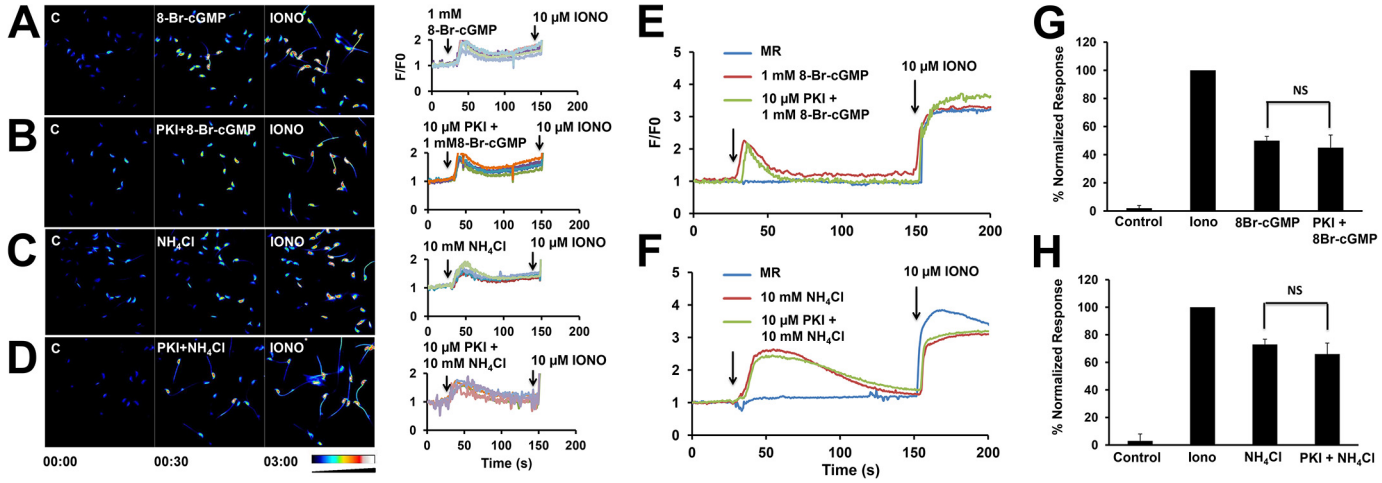

Figure 2. 8-Br-cGMP and NH_4Cl induce $[Ca^{2+}]_i$ increases insensitive to PKA in mouse sperm. Representative fluorescence images from Fluo-3 loaded mouse sperm before additions (*c*, control in *A–D*), after adding 8-Br-cGMP or NH_4Cl in absence or presence of PKI (*middle panels*) and in response to 10 μM ionomycin (*IONO*, positive control in *A–D*). *Right panels* show four to five representative single cell fluorescence traces under the different experimental conditions described in the *left middle panels*. *A*, addition of 8-Br-cGMP increases $[Ca^{2+}]_i$. *B*, as anticipated, PKI (10 μM) does not inhibit the 8-Br-cGMP response. *C*, NH_4Cl 10 mM also elevates $[Ca^{2+}]_i$. *D*, PKI (10 μM) does not inhibit the NH_4Cl response. Panel *C* is also included in Fig. S1*C*. Notably, preincubation of sperm with 10 μM PKI does not affect the $[Ca^{2+}]_i$ increases triggered by either 8-Br-cGMP or NH_4Cl, demonstrating the high specificity of PKI for PKA. *E*, average fluorescence traces from sperm (~150 cells) of four different mice subjected to the experimental conditions as in *A* and *B*. *F*, average traces from sperm from four different mice under the experimental conditions shown in *C* and *D*. *G*, summary plot of normalized maximum $[Ca^{2+}]_i$ increase responses shown in *E*. *H*, summary plot of normalized $[Ca^{2+}]_i$ maximum increases obtained in *F*. *ns*, not significant.

the EGTA-induced depolarization was due mainly to this CatSper property and the amplitude of this response can be used to evaluate CatSper activity in a variety of conditions. Consistently, CatSper inhibitors blocked the EGTA-induced response (24, 28). Although indirect, this assay has the advantage of being straightforward and it is useful to design more demanding electrophysiological experiments. Therefore, to evaluate CatSper activity, Em of noncapacitated sperm was measured with a fluorescent cyanine dye before and after adding 3.5 mM EGTA to suddenly decrease external $[Ca^{2+}]$ below 30 nM in the external media. As a result, the sperm resting Em (−45 mV) was significantly depolarized as Na^+ influx occurs mainly through CatSper. As predicted, the depolarizing response to EGTA was Na^+-dependent (Fig. S2, *A–D*).

As HCO_3^- activates Adcy10, to analyze the extent by which the cAMP pathway was involved in CatSper regulation, we first

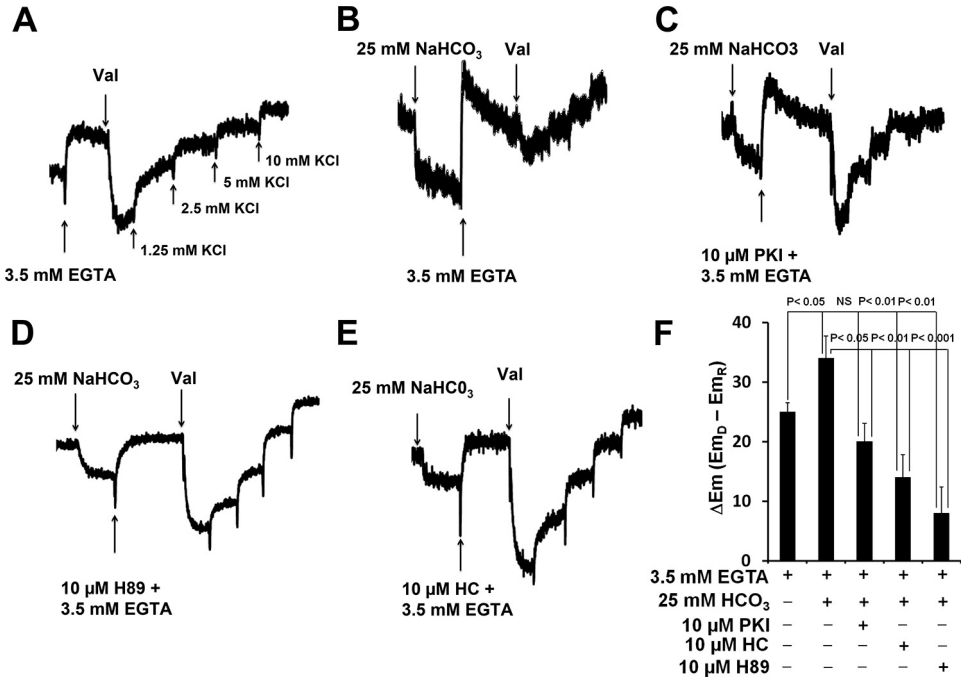

Figure 3. PKI, a specific PKA-inhibitor; H89, another PKA-inhibitor; and HC, a CatSper blocker, inhibit the HCO_3^- induced stimulation of the Em depolarization triggered by EGTA. The Em of cauda sperm was measured with a fluorescent cyanine dye using the CatSper activity protocol, described previously. *A*, representative fluorescence trace obtained in control (basal Em) and after addition of 3.5 mM EGTA. The upward signal indicates an Em depolarization caused by Na^+ influx through CatSper channels. Em calibration involves adding 1 μM valinomycin and sequential and incremental K^+ concentrations of 1.25, 2.5, 5, and 10 mM, indicated only in *A* by *arrows*. *B*, initial addition of 25 mM HCO_3^- hyperpolarizes in the presence of 1.7 mM Ca^{2+}. Thereafter, addition of 3.5 mM EGTA depolarizes Em unveiling CatSper activity in the presence of HCO_3^-. *C*, preincubation (5 min) with 10 μM PKI (specific PKA inhibitor), in an experiment as in *B*, significantly decreases the depolarization induced by 3.5 mM EGTA. *D*, preincubation (5 min) with H89, another PKA inhibitor, also decreases the depolarization induced by 3.5 mM EGTA. *E*, preincubation (5 min) with 10 μM HC (CatSper blocker) significantly diminishes the Em depolarization caused by adding 3.5 mM EGTA. *F*, summary plot of experiments in *A–D*, showing the average differences between Em + compound (Em_D) minus Em resting (Em_R), corrected by the initial HCO_3^- induced hyperpolarization (ΔEm ($Em_D - Em_R$)).

assayed the effect of adding 25 mM HCO_3^- to sperm on the EGTA-induced depolarization amplitude (Fig. 3*A*). Previously, we had shown that HCO_3^- addition induced Em hyperpolarization in sperm (Fig. 3*B*) (4). Once fluorescence reached the new steady state, EGTA was added and the depolarization amplitude measured. The experiments show that the EGTA-induced depolarization was increased when sperm were previously exposed to HCO_3^- (Fig. 3*B*). Furthermore, 10 μM of PKI (Fig. 3*C*) and H89 (Fig. 3*D*), two PKA inhibitors, essentially eliminated the HCO_3^- stimulation. Confirming that EGTA-induced depolarization is mainly because of CatSper, 10 μM HC-056456 (HC), a CatSper blocker (29), inhibited the HCO_3^- stimulated response (Fig. 3*E*). A summary of these experiments is presented in Fig. 3*F* showing the average differences between Em + compound (Em_D) minus Em resting, corrected by the initial HCO_3^- induced hyperpolarization.

Bicarbonate increases CatSper activity by stimulating PKA

The results described above on the effects of HCO_3^- and cAMP on $[Ca^{2+}]_i$, and of HCO_3^- on the amplitude of the EGTA-induced depolarization, as well as their inhibition by PKI and H89, suggest that PKA may be involved in the regulation of CatSper. To further evaluate this hypothesis, we conducted whole cell patch clamp electrophysiological measurements by attaching a patch pipette to the sperm plasma membrane cytoplasmic droplet (30). As indicated earlier, CatSper monovalent currents can be measured by reducing divalent cations from the recording media to less than 30 nM (30). These monovalent currents are because of the permeation of Na^+ and Cs^+ ions. For these experiments, we used a voltage ramp protocol from −80 to +80 mV (Fig. 4*A*). In these conditions, we measured typical monovalent CatSper currents obtained in control conditions and after perfusing HCO_3^- (25 mM) in the same sperm (Fig. 4*B*). Results from five independent experiments indicate a significant HCO_3^--induced increase in $I_{CatSper}$ currents (Fig. 4*C*). In addition, the HCO_3^--induced increase of these currents was suppressed with the CatSper inhibitor HC (Fig. 4, *D* and *E*).

It is known that the addition of HCO_3^- may lead to a pH_i increase either directly or possibly mediated by the sperm-specific Na^+/H^+ exchanger stimulated by hyperpolarization or by the rise in cAMP (4, 31, 32). To discard these possibilities $I_{CatSper}$ was recorded substituting external Na^+ for Cs^+ because Na^+/H^+ exchangers do not operate with Cs^+ (33) and, as in other experiments, including 20 mM HEPES in the internal solution for buffering pH_i changes. Under these conditions, an Na^+-free medium, the possible pH_i increase induced by HCO_3^-, is effectively eliminated; however, when the cell was exposed to HCO_3^-, $I_{CatSper}$ increased (Fig. 4*F*). These findings, summarized in Fig. 4*G*, indicate that the stimulation caused by HCO_3^- is not because of any pH_i increase it could cause. Finally, the role of CatSper mediating the HCO_3^--induced current stimulation was further analyzed using sperm from CatSper null mice. In sperm from the null mice, the stimulatory effect of HCO_3^- in current measurements was not observed

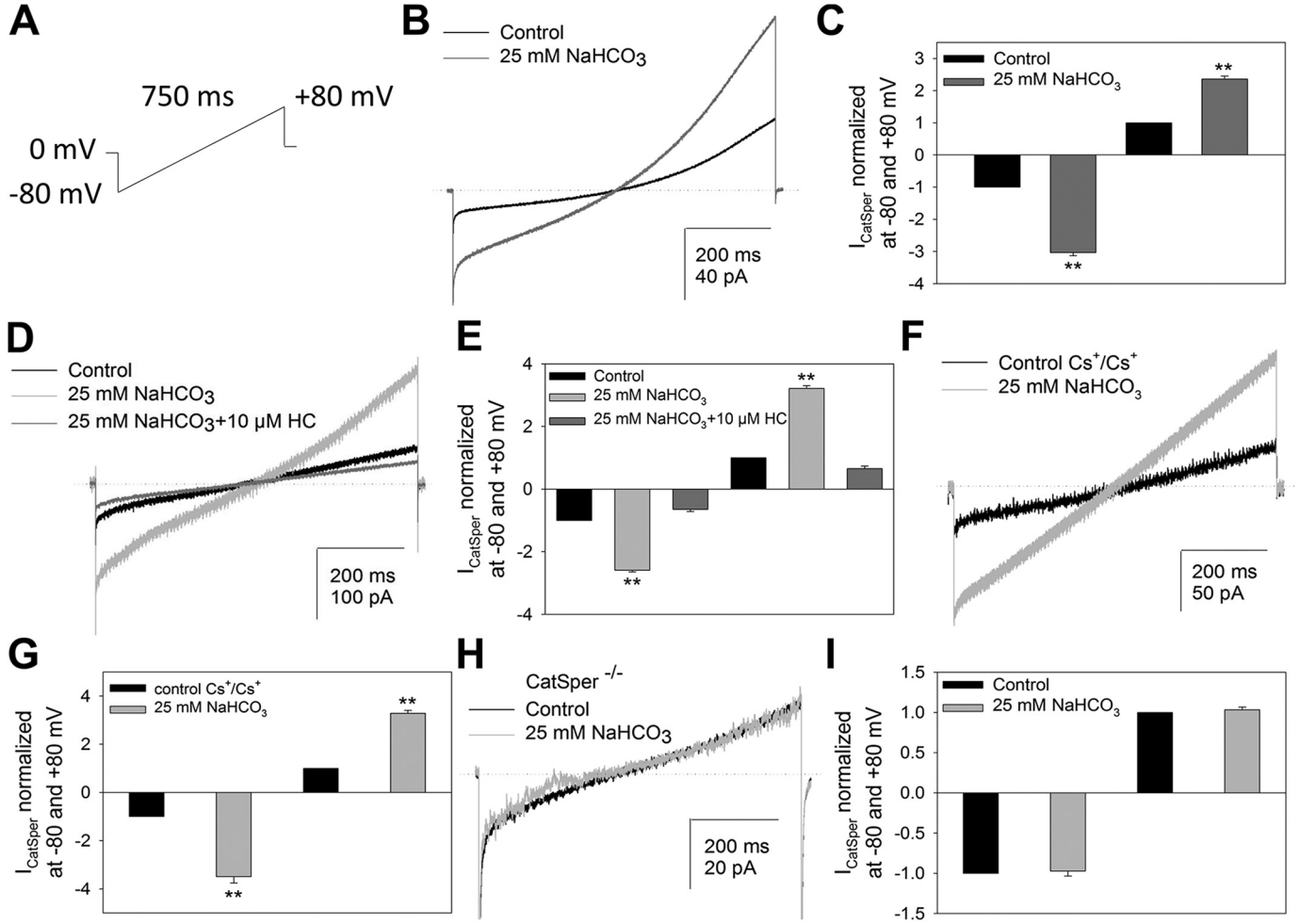

Figure 4. Bicarbonate strongly potentiates monovalent CatSper current in mouse sperm. *A*, typical voltage-ramp protocol used for recording monovalent CatSper current in whole-cell voltage-clamp experiments. *B*, representative monovalent whole cell CatSper current ($I_{CatSper}$) recorded from a mouse spermatozoon in the absence (*black trace*) and presence (*dark gray trace*) of 25 mM HCO_3^- under divalent cation-free solutions. Note the evident increase of current obtained in presence of HCO_3^-. *C*, relative current amplitudes plotted under control and HCO_3^- conditions measured at −80 and +80 mV from experiments as shown in *B*. Bicarbonate clearly potentiates the inward and outward $I_{CatSper}$. The data plotted are the mean ± S.E. of six sperm each from a different mouse. *D*, representative $I_{CatSper}$ obtained from the same spermatozoon in three different conditions: control (*black trace*), HCO_3^- (*gray*), and HCO_3^- plus 10 μM HC (*dark gray*). *E*, normalized current amplitudes with respect to control measurement at −80 and +80 mV under the different experimental conditions shown in *D*. The presence of CatSper blocker HC completely inhibited the effect of HCO_3^-. *F*, representative $I_{CatSper}$ recorded from the same spermatozoon under symmetrical Cs^+ condition in control (*black trace*) and after addition of HCO_3^- (*gray trace*). HCO_3^- induced the equivalent increase of $I_{CatSper}$ as in *B*. *G*, $I_{CatSper}$ normalized with respect to control measurement at −80 and +80 mV under control and HCO_3^- conditions. The data plotted are mean ± S.E. of five different sperm, each from a different mouse. *H*, representative monovalent $I_{CatSper}$ recorded from a spermatozoon obtained from a CatSper null mouse under two different experimental conditions: in absence (control, *black trace*) and presence of 25 mM HCO_3^- (*gray trace*). *I*, summary of $I_{CatSper}$ normalized amplitudes measured at −80 and +80 mV without and with of 25 mM HCO_3^-. Note that HCO_3^- is unable to stimulate the current under CatSper conditions in sperm from CatSper null mice. The data plotted are mean ± S.E. of four sperm each from a different mouse.

(Fig. 4, *H* and *I*). Altogether, these results indicate that the HCO_3^--induced increase in currents are mediated by CatSper.

The intracellular cAMP/PKA pathway contributes to $I_{CatSper}$ stimulation

If HCO_3^- stimulates $I_{CatSper}$ through the action of Adcy10 and the cAMP pathway, its effect should be inhibited by PKI, which specifically eliminates PKA activity. Therefore, sperm were exposed to PKI (10 μM) and then HCO_3^- was added. In these conditions, the HCO_3^--induced $I_{CatSper}$ stimulation was completely inhibited (Fig. 5, *A* and *B*). On the other hand, as described by others (30, 34), addition of NH_4Cl (10 mM) significantly stimulated $I_{CatSper}$ currents (Fig. 5*C*). However, contrary to the addition of HCO_3^-, the NH_4Cl stimulatory effect was not abrogated in the presence of PKI (10 μM) (Fig. 5*D*). These loss of function experiments strongly suggest that the HCO_3^- effect on $I_{CatSper}$ is mediated by PKA.

To further test this possibility, gain of function experiments using cAMP agonists were conducted. It has been proposed that the effect of chemically modified permeable cyclic nucleotides on human CatSper is not because of the cyclic nucleotide part of the molecule but to the chemical moiety attached to the nucleotide acting externally on the channel and not through intracellular pathways. Therefore, to test that cAMP is acting inside, the nucleotide was directly introduced into the sperm through the patch clamp pipette. Initially, we tested 1 mM cAMP (not shown) and thereafter found that 100 μM elicited a similar response. To prevent cAMP degradation, the bath solution contained the phosphodiesterase inhibitor IBMX (100 μM). Under these conditions $I_{CatSper}$ was stimulated

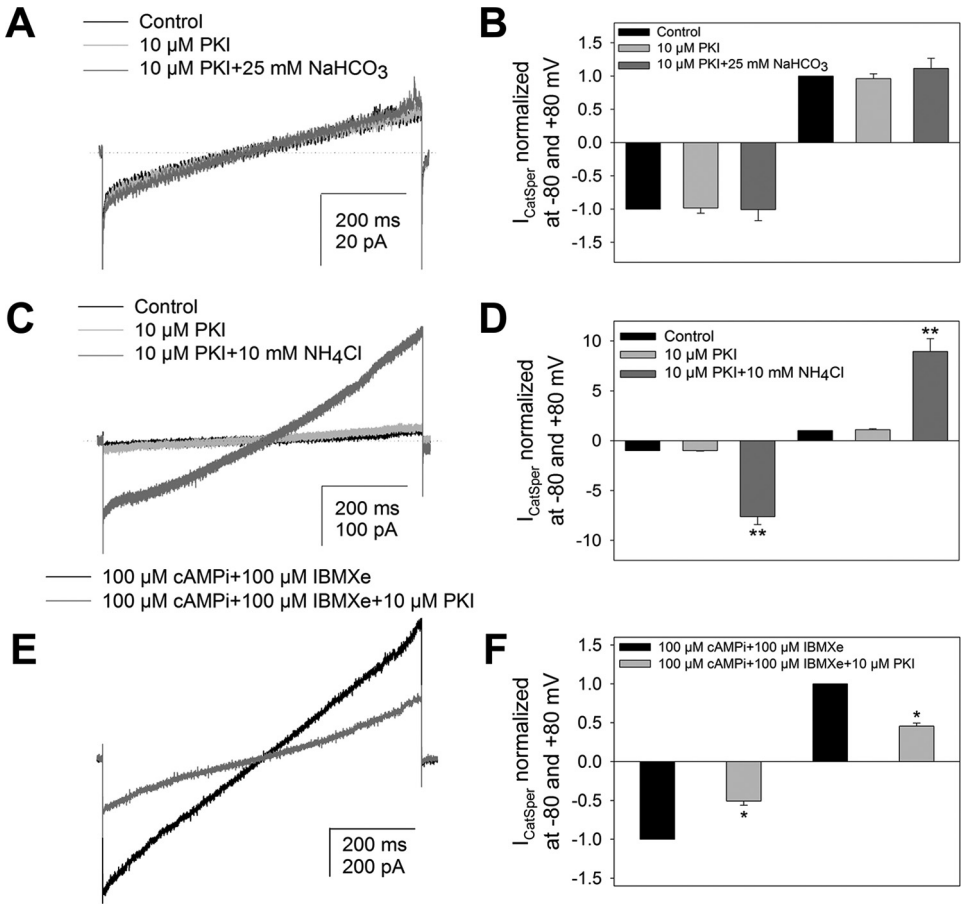

Figure 5. The cAMP/PKA pathway contributes to $I_{CatSper}$ stimulation. Ramp-voltage protocol is the same as shown in Fig. 4*A*. *A*, representative monovalent $I_{CatSper}$ recorded from the same spermatozoon under three different conditions: control (*black trace*), in presence 10 μM PKI (*gray trace*), and 10 μM PKI plus 25 mM HCO_3^- (*dark gray trace*). The presence of PKI completely inhibited the HCO_3^--induced stimulation of $I_{CatSper}$. *B*, $I_{CatSper}$ normalized with respect to control condition measured at −80 and +80 mV under the conditions shown in *A*. The data plotted are the mean ± S.E. obtained from five sperm each from a different mouse. *C*, representative monovalent $I_{CatSper}$ recorded from a spermatozoon under three different conditions: control (*black trace*), 10 μM PKI (*gray trace*), and 10 μM PKI plus 10 mM NH_4Cl (*dark gray trace*). The presence of PKI fails to prevent the stimulation of $I_{CatSper}$ by an alkalinization. *D*, $I_{CatSper}$ normalized with respect to control conditions measured at −80 and +80 mV under the experimental conditions shown in *C*. The data plotted are the mean ± S.E. from five sperm each from a different mouse. *E*, representative monovalent $I_{CatSper}$ obtained in two different conditions: control (*black trace*) and with 100 μM of cAMP inside the pipette solution and 100 μM IBMX in the bath solution (*gray trace*). Note that the amplitude of current in presence of cAMP and IBMX is higher than current obtained in control condition. *F*, $I_{CatSper}$ normalized amplitudes were measured at −80 and +80 mV from original current traces recorded in different spermatozoa obtained from five mice. Clearly, $I_{CatSper}$ is potentiated in presence of cAMP.

by 100 μM cAMP (Fig. 5, *E* and *F*). Again, if PKA mediates the cAMP stimulation of $I_{CatSper}$, it would be expected that PKI would inhibit this response, and indeed it does (Fig. 5, *E* and *F*).

In another set of experiments we tested H89, another PKA inhibitor. The addition of 10 μM of H89 inhibited $I_{CatSper}$ previously stimulated by 25 mM of HCO_3^- (Fig. 6, *A* and *B*). As expected, H89 also inhibited $I_{CatSper}$ stimulated by cAMP inside the pipette. Consistent with our results measuring $[Ca^{2+}]_i$, adding H89 was also able to eliminate the $I_{CatSper}$ stimulated by alkalinization with 10 mM of NH_4Cl (Fig. 6, *C* and *D*).

The unexpected inhibition of the NH_4Cl-induced stimulation of $I_{CatSper}$ suggested an additional target (Fig. 6, *E* and *F*). To contend with this lack of specificity we examined the effect of Rp-cAMPS, a membrane-permeable and specific inhibitor of the activation by cAMP of cAMP-dependent protein kinase I and II. This analog binds to the PKA regulatory subunit and prevents its dissociation from the catalytic subunit and is also resistant toward cyclic nucleotide phosphodiesterases (35, 36). This mode of inhibition differs from that of PKI, which is a competitive inhibitor of the catalytic subunit.

We found that Rp-cAMPS inhibited the stimulation of the current by HCO_3^- (Fig. 7, *A* and *B*). Nevertheless, the addition of Rp-cAMPS did not prevent the stimulatory effect of NH_4Cl (Fig. 7, *C* and *D*). This result strengthens our hypothesis that the PKA pathway participates in the activation of $I_{CatSper}$.

During capacitation, sperm are exposed to high HCO_3^- concentrations that elevate cAMP via sAC stimulation and activate the PKA pathway. Here we presented evidence consistent with the proposal that PKA is able to stimulate CatSper directly or through another protein it phosphorylates (Fig. 8). The model shows that in addition to voltage and pH alkalinization, CatSper can also be activated by a PKA-dependent phosphorylation event.

Discussion

Sperm gain the ability to fertilize metaphase II–arrested eggs in the female tract in a process known as capacitation. At the molecular level, capacitation is initiated as soon as spermatozoa are exposed to HCO_3^- anions which stimulate Adcy10 and produce a fast elevation of cAMP levels. In addition to cAMP,

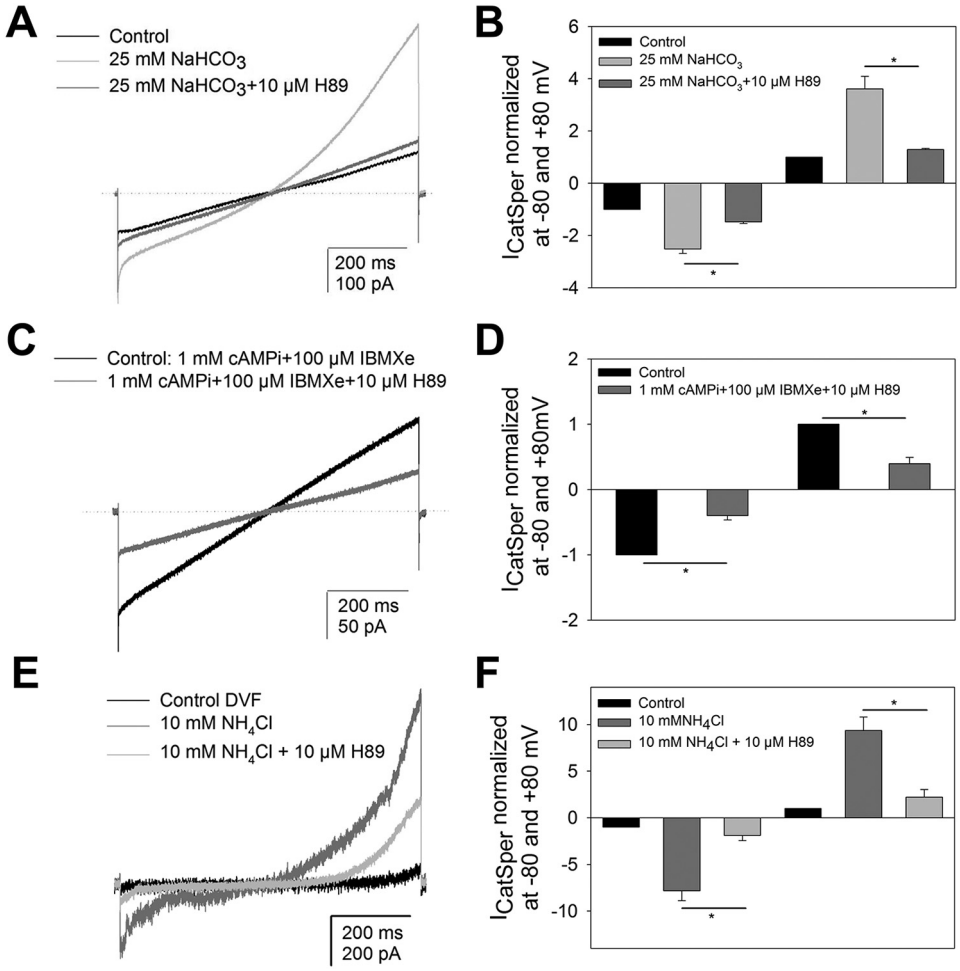

Figure 6. H89 inhibits the HCO_3^-- and cAMP-induced stimulation of $I_{CatSper}$. *A*, representative monovalent $I_{CatSper}$ obtained in three different conditions: control (*black trace*), in presence of 25 mM of HCO_3^- (*gray trace*), and after addition of 10 μM H89 (*dark gray trace*). Note that the amplitude of the HCO_3^- stimulated current is inhibited by H89 almost to the control level. *B*, $I_{CatSper}$ normalized amplitudes were measured at −80 and +80 mV from original current traces recorded in different spermatozoa obtained from five mice. Clearly, $I_{CatSper}$ is potentiated by HCO_3^- and significantly inhibited by H89. *C*, representative monovalent $I_{CatSper}$ obtained in two different conditions: with 1 mM of cAMP inside the pipette solution and 100 μM IBMX in the bath solution (*black trace*), and after addition of 10 μM of H89 (*gray trace*). Clearly, the amplitude of current in presence of cAMP and IBMX is decreased upon H89 addition. *D*, $I_{CatSper}$ normalized amplitudes were measured at −80 and +80 mV from original current traces such as shown in *C*, recorded in different spermatozoa obtained from five mice. *E*, representative monovalent $I_{CatSper}$ obtained in three different conditions: control (*black trace*), in presence of 10 mM NH_4Cl (*dark gray trace*), and after addition of 10 μM of H89 (*gray trace*). Note that the amplitude of current in presence of NH_4Cl is potentiated and when H89 is added it is significantly diminished. *F*, $I_{CatSper}$ normalized amplitudes were measured at −80 and +80 mV from original current traces recorded in different spermatozoa obtained from five mice as show in *E*. Although not completely, H89 significantly inhibits the $I_{CatSper}$ stimulation caused by NH_4Cl.

sperm capacitation is also associated with an increase in $[Ca^{2+}]_i$. Although several Ca^{2+} channels have been proposed to be present in mammalian sperm (13, 37, 38), only two of them have been conclusively shown to be present in these cells using electrophysiological recordings combined with knockout genetic models (30, 39, 40). One of them is the purinergic receptor P2X2 (40). The second is the Ca^{2+} channel complex CatSper (18). Whereas P2X2 KO mice are fertile, lack of CatSper results in complete sterility (14, 41, 42). Recently, we have shown that the lack of hyperactivation and infertility phenotypes can be overcome elevating $[Ca^{2+}]_i$ pharmacologically by exposing CatSper KO sperm to A23187 for a short period of time (43). Although the role of CatSper is well established in sperm function, how this channel complex is regulated is still not fully understood.

As first described by Weyand's lab (44), it is well established that cGMP and cAMP permeable agonists induce $[Ca^{2+}]_i$ elevation in mammalian sperm. Moreover, in bovine sperm, caged cyclic nucleotides were shown to increase $[Ca^{2+}]_i$ (44, 45). Originally, this effect was attributed to the presence of a testis-specific transcript of a cyclic nucleotide gated channel (46). Interestingly, the cyclic nucleotide–dependent stimulation of $[Ca^{2+}]_i$ increase was not observed in sperm from CatSper KO mice (18), indicating that this channel complex mediates cyclic nucleotide effects in $[Ca^{2+}]_i$. However, none of the CatSper subunits contain consensus sequences for cyclic nucleotide–binding domains, suggesting that the effect of permeable cyclic nucleotides is not direct.

In a landmark manuscript, Kirichok *et al.* (30) showed that whole cell currents could be recorded in mouse sperm. CatSper was readily recorded in divalent-free external solutions where it efficiently transports monovalent cations such as Na^+ and Cs^+. In this work, the authors did not observe current stimulation by 8-Br-cAMP and 8-Br-cGMP (Fig. S3 in Ref. 30). However, they

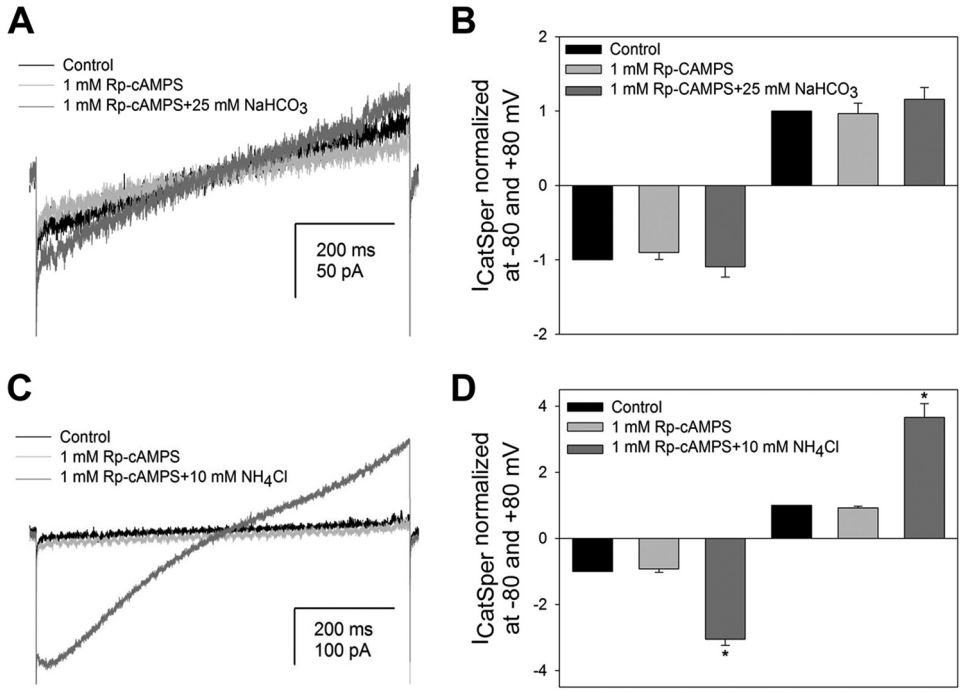

Figure 7. Rp-cAMPS inhibits the HCO_3^--induced stimulation of $I_{CatSper}$. *A*, representative monovalent $I_{CatSper}$ obtained in three different conditions: control (*black trace*), in presence of 1 mM of Rp-cAMPS (*gray trace*), and after addition of 25 mM HCO_3^- (*dark gray trace*). Note that the addition of Rp-cAMPS completely prevents the HCO_3^- effect. *B*, summary of $I_{CatSper}$ normalized amplitudes in conditions as in *A* measured at −80 and +80 mV from original current traces recorded in different spermatozoa obtained from four mice. *C*, representative monovalent $I_{CatSper}$ obtained in three different conditions: control (*black trace*), with 1 mM of Rp-cAMPS (*gray trace*), and after addition of 10 mM of NH_4Cl (*dark gray trace*). Clearly, Rp-cAMPS failed to prevent the NH_4Cl stimulation. *D*, summary of $I_{CatSper}$ normalized amplitudes measured at −80 and +80 mV from original current traces such as show in *C*, recorded in different spermatozoa obtained from four mice. Note that the amplitude of current in presence of NH_4Cl is potentiated although Rp-cAMPS is present.

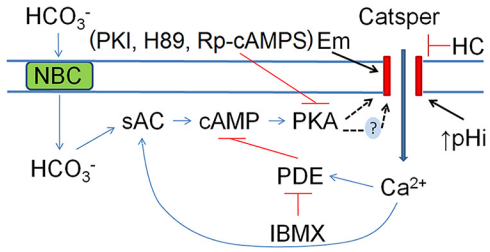

Figure 8. Model for PKA-activated CatSper channel in mouse sperm. During capacitation sperm are exposed to high HCO_3^- concentrations that stimulate, via sAC, cAMP increases which activate PKA that stimulates CatSper, directly or indirectly. *NBC* represents the Na^+/HCO_3^- cotransporter that transports HCO_3^- into the cell. We propose that in addition to voltage and alkaline pH_i, the PKA pathway also contributes to CatSper activation.

performed these experiments in the presence of divalent cations, a condition where the currents are very small. Furthermore, these tests were carried out at pH_i 6, where CatSper is not very active or at pH_i 8, where it is fully active before adding the cyclic nucleotides. Possibly these conditions explain why no changes in the current amplitude were observed.

Other electrophysiological and $[Ca^{2+}]_i$ imaging studies reported that 8-Brc-GMP and 8-Br-cAMP did stimulate mouse monovalent currents and Ca^{2+} uptake. The 8-Br-cGMP response was sensitive to diltiazem, which the authors interpreted as indicating the participation of cyclic nucleotide–gated (CNG) channels. The 8-Br-cGMP response was also inhibited by PKG antagonists, suggesting the involvement of this kinase in their regulation (47, 48). Although small molecular weight inhibitors often have off-target effects on other kinases, these experiments suggest that cyclic nucleotide effects are mediated by phosphorylation.

More recently, the effect of permeable cyclic nucleotides was attributed to binding of the chemically modified cGMP and cAMP to extracellular human but not mouse CatSper domains (22, 30) and not by modulation of intracellular cGMP- or cAMP-dependent pathways. The authors showed that although exogenous addition of 8-Br-cGMP or 8-Br-cAMP elevated $[Ca^{2+}]_i$ when cGMP or 8-Br-cGMP were directly introduced inside the sperm through a patch clamp pipette, these compounds failed to elevate $[Ca^{2+}]_i$. A similar experiment introducing cAMP inside sperm was not reported. Considering that many other compounds with different chemical structure such as odorants, menthol, progesterone, and permeable cyclic nucleotides also stimulate CatSper currents (22); these authors suggested that CatSper can act as a polymodal sensor for chemical cues. Comparative studies between mouse and human CatSper have revealed species-specific differences. Although human CatSper currents can be stimulated indirectly by progesterone (23, 49, 50), this hormone does not activate the mouse CatSper channel complex (49). On the other hand, pH_i alkalinization can directly regulate CatSper activity in both species. Despite these advances, the role of cAMP-dependent pathways in the regulation of CatSper is controversial.

As mentioned in the Introduction, there is also contrasting evidence regarding the ability of HCO_3^- to induced an increase in $[Ca^{2+}]_i$ (18, 19). In this last paper, this response was considered not significant, although observing Fig. 2 in Ref. 19, a

change caused by HCO_3^- can clearly be seen which is not present in sperm from CatSper null mice.

The controversy surrounding the response to permeable analogs of cAMP and cGMP and HCO_3^- in mouse sperm motivated us to reevaluate these matters. To examine our hypothesis that the cAMP/PKA pathway regulates CatSper, this channel complex activity was tested using a battery of assays. First we examined how $[Ca^{2+}]_i$ responded to conditions that increase PKA activity such as addition of HCO_3^- and permeable cAMP agonists. As shown before by several groups (18, 25, 51, 52), 8-Br-cAMP elevated $[Ca^{2+}]_i$ and similar results were observed when HCO_3^- was added in single sperm loaded with Fluo-3, a Ca^{2+} indicator dye. Consistent with our hypothesis, myristoylated PKI peptide, which specifically blocks PKA activity, inhibited both the HCO_3^- and the 8-Br-cAMP responses. On the other hand, PKI did not block the $[Ca^{2+}]_i$ elevation caused by 8-Br-cGMP or by the NH_4Cl-induced pH_i alkalinization. Importantly, the lack of PKI inhibitory effect when $[Ca^{2+}]_i$ elevation was induced by 8-Br-cGMP and NH_4Cl, which do not activate PKA, indicates that the PKI effect is not unspecifically targeting CatSper. To strengthen the evidence indicating the involvement of PKA in the regulation of CatSper, we also used H89, another PKA inhibitor. As anticipated, H89 inhibited the $[Ca^{2+}]_i$ increase induced by 8-Br-cAMP, supporting our hypothesis that CatSper can be regulated through the cAMP/PKA pathway.

CatSper efficiently transports monovalent cations in the absence of external Ca^{2+} (32). Thus, when EGTA is added to sperm in noncapacitating media in sufficient amount to lower external Ca^{2+} to <30 nM, a depolarization results which is indirectly related to CatSper's activity (24, 27). This strategy conveniently allows sperm population studies in multiple conditions before embarking on more time-consuming electrophysiological recordings. Using this methodology, we determined that HCO_3^- enhances the EGTA-induced depolarization and that this response was blocked by either PKI, H89, or HC, a CatSper blocker (29). Our findings are consistent with the hypothesis that PKA-dependent phosphorylation pathways are involved in the regulation of CatSper activity.

To further examine this hypothesis, sperm exposed to noncapacitating conditions were patch clamped and currents measured. As mentioned earlier, CatSper is optimally studied electrophysiologically by recording monovalent currents when divalent cations are eliminated from the recording media (30). Basal currents were recorded from mouse sperm suspended under this condition by applying a voltage ramp. HCO_3^- addition following this first recording induced a significant increase in the observed currents that were blocked in the presence of either PKI, H89, or HC. Because unexpectedly we found H89 also inhibited the NH_4Cl-induced $I_{CatSper}$ stimulation, indicating a certain lack of specificity, we also tested Rp-cAMPS, an additional specific PKA inhibitor. As this inhibitor blocked the HCO_3^- stimulation of $I_{CatSper}$ but did not influence its enhancement by NH_4Cl, the results using Rp-cAMPS support the participation of PKA in the regulation of this channel. Indeed, two specific PKA inhibitors acting by distinct mechanisms, PKI and Rp-cAMPS, significantly diminished the HCO_3^- stimulation of $I_{CatSper}$.

To further establish the target of the HCO_3^- stimulation leading to this current increase, experiments were carried out in sperm from CatSper null mice. As anticipated, this anion was unable to cause a current increase in these sperm suspended in divalent-free media, clearly suggesting that CatSper is the target. Therefore, pharmacological and genetic loss of function experiments are consistent with the hypothesis that PKA-dependent pathways up-regulate CatSper activity. In addition, gain of function experiments showed that introducing cAMP inside the sperm using the patch pipette also induced a significant increase in current amplitude that was blocked by PKI and H89.

All the findings presented here are consistent with our initial hypothesis that HCO_3^- enters sperm, activates sAC, and elevates cAMP which stimulates PKA. Once active, we show that this kinase directly or indirectly regulates CatSper activity by phosphorylation, enhancing its capacity to conduct and elevate $[Ca^{2+}]_i$, a necessary condition for capacitation including hyperactivation and preparation for the acrosome reaction. Our findings support the central role cAMP/PKA and CatSper play in the maturation process required so sperm may fertilize the egg.

Materials and methods

Products and sources were as follows: Protein kinase A inhibitor (PKI) fragment 14–22, myristoylated trifluoroacetate salt, and Rp-adenosine 3′,5′-cyclic monophosphorothioate triethylammonium salt (Rp-cAMPS) (Sigma-Aldrich), and H89 dihydrochloride (Cayman Chemical, Ann Arbor, MI), 3-isobutyl-l-methylxanthine hydrate (IBMX) (Calbiochem), CatSper blocker HC-056456 (VITAS-M Laboratory) (29), 3′,5′-cAMP sodium salt (cAMP) (Sigma-Aldrich), 8-bromoguanosine 3′,5′-cyclic monophosphate sodium salt monohydrate cGMP (Sigma-Aldrich). $NaHCO_3$ and all other salts were from Sigma-Aldrich. In all cases aliquots were diluted and added to the recording solutions and volumes chosen so that the maximum concentration of solvent was at most 1% (v/v).

Sperm manipulation techniques

Animals in general were euthanized in accordance with the Institutional Animal Care and Use Committee (IACUC) guidelines of University of Massachusetts-Amherst and the Institute of Biotechnology/UNAM. Cauda epididymal mouse sperm were collected from CD1 (Charles River Laboratories, Wilmington, MA) retired male breeders by placing minced cauda epididymis in a TYH medium with following composition in mM: 119.3 NaCl, 4.7 KCl, 1.71 $CaCl_2 \cdot 2H_2O$, 1.2 KH_2PO_4, 1.2 $MgSO_4 \cdot 7H_2O$, 0.51 sodium pyruvate, 5.56 glucose, 20 HEPES, and pH 7.4. This medium, which does not support capacitation, was prepared without bovine serum albumin and $NaHCO_3$. After 10 min, sperm in suspension were washed in 10 ml of the same medium by centrifugation at $800 \times g$ for 10 min at room temperature (room temperature = 24 °C). Sperm were then resuspended to a final concentration of 2×10^7 cells/ml and diluted 10 times in the appropriate medium depending on the experiment performed. The pH was maintained at 7.4.

Intracellular calcium ($[Ca^{2+}]_i$) measurements

Aliquots of motile noncapacitated sperm were loaded with 4 μM of the fluorescent Ca^{2+} indicator Fluo-3 AM in the presence of 0.05% pluronic acid for 30 min. Afterward, they were washed once at 2000 rpm/8 min and resuspended in noncapacitating TYH media. Sperm were attached on laminin (1 mg/ml) precoated cover slips, allowing their flagella to move continuously. The coverslip was mounted on a chamber (Harvard Apparatus) and placed on the stage of an inverted microscope (Eclipse TE 300; Nikon). Sperm were exposed to TYH medium alone (MR) for control experiments or to 1 mM 8-Br-cAMP, 10 μM PKI, 1 mM 8-Br-cGMP, 10 mM NH_4Cl for test experiments. Inhibitors such as PKI and H89 (10 μM), were incubated 5 min before adding nucleotides or 10 mM NH_4Cl. As vitality control 10 μM ionomycin was added at the end of each experiment. In these experiments at least 150 individual mouse sperm were analyzed per treatment from each of three different mice. Fluo-3 loaded samples were excited with a Blue LED (3.15 A, Luminus Devices, Woburn, MA), with a band pass excitation (HQ 480/40X) filter, dichroic mirror (Q505lp), and emission (HQ 535/50M) filters (Chroma Technology, Bellows Falls, VT). The LED output was synchronized to the exposure out signal of an iXon 888 CCD camera via the control box to produce a single flash of 2-ms duration per individual exposure. The camera exposure time was set equivalent to the flash duration (2 ms). Images were collected every 500 ms using iQ software (Andor Technology). Images were processed and analyzed with macros written in ImageJ (Version 1.38, National Institutes of Health). Regions of interest were drawn on each sperm head and then analyzed for quantification. A plot was generated in Microsoft Office Excel 2007 (Microsoft). Fluorescence is expressed as F-F0/F0.

Membrane potential measurements

Em measurements were performed following the protocol described previously in detail (4, 27). Briefly, mature sperm from caudal epididymides were collected, diluted in noncapacitating TYH medium, and exposed to a final concentration of 1 μM Em-sensitive dye 3,3′-dipropylthiacarbocyanine iodide ($DiSC_3(5)$) for 5 min. Mitochondrial membrane potential was dissipated with 500 nM carbonyl cyanide *m*-chlorophenylhydrazone (CCCP), and sperm were incubated for 2 additional minutes. After this period, 1.5 ml of the sperm suspension was transferred to a gently stirred cuvette at 37 °C and the fluorescence monitored using an Ocean Optics USB4000 spectrofluorometer operated by Spectra Suite (Ocean Optics, Largo, FL) at 620/670 nm excitation/emission wavelength pair (27). Cell hyperpolarization decreases the dye fluorescence. Recordings were initiated after reaching steady-state fluorescence (1–3 min) and were converted to Em as described previously (27). Calibration was performed by adding 1 μM valinomycin and sequential additions of KCl. The equilibrium potential for K^+ was calculated with the Nernst equation considering intracellular mouse sperm K^+ is 120 mM.

Caudal sperm preparation for electrophysiology

Cauda epididymal sperm were obtained from CD-1 WT and from C57BL/6 CatSper1 KO mice for swim out in noncapacitating TYH medium. Sperm were stored in physiological solution (HS) with the following composition in mM: 135 NaCl, 5 KCl, 2 $CaCl_2$, 1 $MgSO_4$, 10 lactic acid, 1 pyruvic acid, 5 glucose, 20 HEPES, pH 7.4, at 4 °C until assayed. At the desired time, 100 μl aliquots of the cell suspension were dispensed into a recording chamber (1 ml total volume) and subjected to electrophysiological recording.

Electrophysiology

Whole-cell macroscopic currents were obtained by patch clamping the sperm cytoplasmic droplet (30). All recordings were performed using a patch clamp amplifier (Axopatch 200, Molecular Devices) at room temperature (22 °C). Pulse protocols, data acquisition, and data storage were performed using pCLAMP6 software (Molecular Devices) and data analysis was carried out with Clampfit 10.6 (Molecular Devices), Origin 7.5 (Microcal Software), and Sigma Plot 10 (Systat Software). Current records, unless indicated otherwise, were acquired at 20–100 kHz and filtered at 2–5 kHz (internal four-pole Bessel filter) using a computer attached to a DigiData 1200 (Molecular Devices). Patch pipettes were pulled from borosilicate glass (Kimble; Queretaro, México) and had a final resistance between 15 and 20 megaohms. Initial experiments were carried out using physiological solutions (HS) in the bath and the pipette solution contained in mM: 110 Met-K, 30 KCl, 10 NaCl, 1 ATP-Mg, 1 $CaCl_2$, 10 EGTA, 10 HEPES, pH 6.8. For recording CatSper currents we used a CatSper-recording solution, also called divalent cation-free solutions by Kirichok *et al.* (30); the bath solution contained in mM: 150 sodium gluconate, 2 Na_2EDTA, 2 EGTA, 20 HEPES, pH 7.4, and the pipette solution contained in mM: 135 Cs-$MeSO_3$, 5 CsCl, 5 Na-ATP, 10 EGTA, 20 HEPES, pH 7.0. The osmolarity of all solutions was adjusted with dextrose. The total currents under physiological conditions were recorded applying a voltage-step protocol from −100 mV to +200 mV in 10-mV increments with a holding potential of 0 mV and lasting the time indicated in the figures. For CatSper current ($I_{CatSper}$) recording we used a conventional voltage-ramp protocol from −80 mV to +80 mV with duration of 750 ms from a holding potential of 0 mV. Seals between the patch pipette and the cytoplasmic droplet in sperm were formed in HS bath solution and after achieving the whole cell configuration the bath solution could be changed for divalent cation-free solution.

Data analysis

Data are given as mean ± S.E. In all cases, differences between raw experimental and control data were tested by Student's *t* tests if not otherwise stated. Differences were considered significant when *, $p < 0.05$; **, $p < 0.01$; and ***, $p < 0.001$.

Author contributions—G. O. investigation; J. L. d. l. V.-B. writing-original draft; A. D. funding acquisition; G. O. designed, performed, and analyzed the patch clamp sperm experiments, discussed the data, and prepared the manuscript; J. L. d. l. V.-B. designed, performed, and analyzed calcium imaging and membrane potential experiments; D. H. did experiments and participated in data discussion.; C. M. S. provided CatSper KO mice, planned and discussed the data; P. E. V. conceived and coordinated the study and wrote the paper; A. D. conceived and coordinated the study and wrote the paper.

Acknowledgments—We acknowledge Shirley Ainsworth for technical assistance and the staff of the Animal Facilities, Elizabeth Mata, Graciela Cabeza, and Sergio González, and Omar Arriaga from the Computing Unit of IBT UNAM. We thank Drs. Christopher Wood, Ignacio López, and Julio Chávez for suggestions after reading the manuscript.

References

1. Chang, M. C. (1951) Fertilizing capacity of spermatozoa deposited into the fallopian tubes. *Nature* **168,** 697–698 Medline
2. Austin, C. R. (1951) Observations on the penetration of the sperm in the mammalian egg. *Aust. J. Sci. Res.* **4,** 581–596 Medline
3. Burton, K. A., and McKnight, G. S. (2007) PKA, germ cells, and fertility. *Physiology* **22,** 40–46 CrossRef Medline
4. Demarco, I. A., Espinosa, F., Edwards, J., Sosnik, J., de la Vega-Beltrán, J. L., Hockensmith, J. W., Kopf, G. S., Darszon, A., and Visconti, P. E. (2003) Involvement of a Na^+/HCO_3^- cotransporter in mouse sperm capacitation. *J. Biol. Chem.* **278,** 7001–7009 CrossRef Medline
5. Visconti, P. E., Bailey, J. L., Moore, G. D., Pan, D. Y., Olds-Clarke, P., and Kopf, G. S. (1995) Capacitation of mouse spermatozoa.1. Correlation between the capacitation state and protein-tyrosine phosphorylation. *Development* **121,** 1129–1137 Medline
6. Visconti, P. E., Moore, G. D., Bailey, J. L., Leclerc, P., Connors, S. A., Pan, D., Olds-Clarke, P., and Kopf, G. S. (1995) Capacitation of mouse spermatozoa. II. Protein tyrosine phosphorylation and capacitation are regulated by a cAMP-dependent pathway. *Development* **121,** 1139–1150 Medline
7. Esposito, G., Jaiswal, B. S., Xie, F., Krajnc-Franken, M. A., Robben, T. J., Strik, A. M., Kuil, C., Philipsen, R. L., van Duin, M., Conti, M., and Gossen, J. A. (2004) Mice deficient for soluble adenylyl cyclase are infertile because of a severe sperm-motility defect. *Proc. Natl. Acad. Sci. U.S.A.* **101,** 2993–2998 CrossRef Medline
8. Hess, K. C., Jones, B. H., Marquez, B., Chen, Y., Ord, T. S., Kamenetsky, M., Miyamoto, C., Zippin, J. H., Kopf, G. S., Suarez, S. S., Levin, L. R., Williams, C. J., Buck, J., and Moss, S. B. (2005) The "soluble" adenylyl cyclase in sperm mediates multiple signaling events required for fertilization. *Dev. Cell* **9,** 249–259 CrossRef Medline
9. Nolan, M. A., Babcock, D. F., Wennemuth, G., Brown, W., Burton, K. A., and McKnight, G. S. (2004) Sperm-specific protein kinase A catalytic subunit Cα2 orchestrates cAMP signaling for male fertility. *Proc. Natl. Acad. Sci. U.S.A.* **101,** 13483–13488 CrossRef Medline
10. Jansen, V., Alvarez, L., Balbach, M., Strünker, T., Hegemann, P., Kaupp, U. B., and Wachten, D. (2015) Controlling fertilization and cAMP signaling in sperm by optogenetics. *Elife* **4** CrossRef Medline
11. Navarrete, F. A., García-Vázquez, F. A., Alvau, A., Escoffier, J., Krapf, D., Sánchez-Cárdenas, C., Salicioni, A. M., Darszon, A., and Visconti, P. E. (2015) Biphasic role of calcium in mouse sperm capacitation signaling pathways. *J. Cell. Physiol.* **230,** 1758–1769 CrossRef Medline
12. Fraser, L. R. (1987) Minimum and maximum extracellular Ca^{2+} requirements during mouse sperm capacitation and fertilization *in vitro*. *J. Reprod. Fertil.* **81,** 77–89 CrossRef Medline
13. Darszon, A., Nishigaki, T., Beltran, C., and Treviño, C. L. (2011) Calcium channels in the development, maturation, and function of spermatozoa. *Physiol. Rev.* **91,** 1305–1355 CrossRef Medline
14. Lishko, P. V., Kirichok, Y., Ren, D. J., Navarro, B., Chung, J. J., and Clapham, D. E. (2012) The control of male fertility by spermatozoan ion channels. *Annu. Rev. Physiol.* **74,** 453–475 CrossRef Medline
15. Bhoumik, A., Saha, S., Majumder, G. C., and Dungdung, S. R. (2014) Optimun calcium concentration: A crucial factor in regulating sperm motility *in vitro*. *Cell Biochem. Biophys.* **70,** 1177–1183 CrossRef Medline
16. Suarez, S. S. (2008) Regulation of sperm storage and movement in the mammalian oviduct. *Int. J. Dev. Biol.* **52,** 455–462 CrossRef Medline
17. Tateno, H., Krapf, D., Hino, T., Sánchez-Cárdenas, C., Darszon, A., Yanagimachi, R., and Visconti, P. E. (2013) Ca^{2+} ionophore A23187 can make mouse spermatozoa capable of fertilizing *in vitro* without activation of cAMP-dependent phosphorylation pathways. *Proc. Natl. Acad. Sci. U.S.A.* **110,** 18543–18548 CrossRef Medline
18. Ren, D., Navarro, B., Perez, G., Jackson, A. C., Hsu, S., Shi, Q., Tilly, J. L., and Clapham, D. E. (2001) A sperm ion channel required for sperm motility and male fertility. *Nature* **413,** 603–609 CrossRef Medline
19. Carlson, A. E., Westenbroek, R. E., Quill, T., Ren, D., Clapham, D. E., Hille, B., Garbers, D. L., and Babcock, D. F. (2003) CatSper1 required for evoked Ca^{2+} entry and control of flagellar function in sperm. *Proc. Natl. Acad. Sci. U.S.A.* **100,** 14864–14868 CrossRef Medline
20. Qi, H., Moran, M. M., Navarro, B., Chong, J. A., Krapivinsky, G., Krapivinsky, L., Kirichok, Y., Ramsey, I. S., Quill, T. A., and Clapham, D. E. (2007) All four CatSper ion channel proteins are required for male fertility and sperm cell hyperactivated motility. *Proc. Natl. Acad. Sci. U.S.A.* **104,** 1219–1223 CrossRef Medline
21. Chung, J. J., Miki, K., Kim, D., Shim, S. H., Shi, H. F., Hwang, J. Y., Cai, X. J., Iseri, Y., Zhuang, X. W., and Clapham, D. E. (2017) CatSperζ regulates the structural continuity of sperm Ca^{2+} signaling domains and is required for normal fertility. *Elife* **6** CrossRef Medline
22. Brenker, C., Goodwin, N., Weyand, I., Kashikar, N. D., Naruse, M., Krähling, M., Müller, A., Kaupp, U. B., and Strünker, T. (2012) The CatSper channel: A polymodal chemosensor in human sperm. *EMBO J.* **31,** 1654–1665 CrossRef Medline
23. Strünker, T., Goodwin, N., Brenker, C., Kashikar, N. D., Weyand, I., Seifert, R., and Kaupp, U. B. (2011) The CatSper channel mediates progesterone-induced Ca^{2+} influx in human sperm. *Nature* **471,** 382–386 CrossRef Medline
24. Ernesto, J. I., Munoz, M. W., Battistone, M. A., Vasen, G., Martinez-Lopez, P., Orta, G., Figueiras-Fierro, D., de la Vega-Beltran, J. L., Moreno, I. A., Guidobaldi, H. A., Giojalas, L., Darszon, A., Cohen, D. J., and Cuasnicu, P. S. (2015) CRISP1 as a novel CatSper regulator that modulates sperm motility and orientation during fertilization. *J. Cell Biol.* **210,** 1213–1224 CrossRef Medline
25. Liu, J., Xia, J., Cho, K. H., Clapham, D. E., and Ren, D. (2007) CatSperβ, a novel transmembrane protein in the CatSper channel complex. *J. Biol. Chem.* **282,** 18945–18952 CrossRef Medline
26. Liao, Z. D., St. Clair, J. R., Larson, E. D., and Proenza, C. (2011) Myristoylated peptides potentiate the funny current (I_f) in sinoatrial myocytes. *Channels* **5,** 115–119 CrossRef Medline
27. Espinosa, F., and Darszon, A. (1995) Mouse sperm membrane potential: Changes induced by Ca^{2+}. *FEBS Lett.* **372,** 119–125 CrossRef Medline
28. Torres-Flores, V., Picazo-Juárez, G., Hernández-Rueda, Y., Darszon, A., and González-Martínez, M. T. (2011) Sodium influx induced by external calcium chelation decreases human sperm motility. *Hum. Reprod.* **26,** 2626–2635 CrossRef Medline
29. Carlson, A. E., Burnett, L. A., del Camino, D., Quill, T. A., Hille, B., Chong, J. A., Moran, M. M., and Babcock, D. F. (2009) Pharmacological targeting of native CatSper channels reveals a required role in maintenance of sperm hyperactivation. *PLoS One* **4,** e6844 CrossRef Medline
30. Kirichok, Y., Navarro, B., and Clapham, D. E. (2006) Whole-cell patch-clamp measurements of spermatozoa reveal an alkaline-activated Ca^{2+} channel. *Nature* **439,** 737–740 CrossRef Medline
31. Zeng, Y., Oberdorf, J. A., and Florman, H. M. (1996) pH regulation in mouse sperm: Identification of Na(+)-, Cl(−)-, and HCO3(−)-dependent and arylaminobenzoate-dependent regulatory mechanisms and characterization of their roles in sperm capacitation. *Dev. Biol.* **173,** 510–520 CrossRef Medline
32. Wang, D., Hu, J., Bobulescu, I. A., Quill, T. A., McLeroy, P., Moe, O. W., and Garbers, D. L. (2007) A sperm-specific Na+/H+ exchanger (sNHE) is critical for expression and *in vivo* bicarbonate regulation of the soluble adenylyl cyclase (sAC). *Proc. Natl. Acad. Sci. U.S.A.* **104,** 9325–9330 CrossRef Medline
33. Clinescu, O., and Fendler, K. (2015) A universal mechanism for transport and regulation of CPA sodium proton exchangers. *Biol. Chem.* **396,** 1091–1096 CrossRef Medline
34. Lishko, P. V., and Kirichok, Y. (2010) The role of Hv1 and CatSper channels in sperm activation. *J. Physiol.* **588,** 4667–4672 CrossRef
35. Rothermel, J. D., Perillo, N. L., Marks, J. S., and Botelho, L. H. P. (1984) Effects of the specific cAMP antagonist, (Rp)-adenosine cyclic 3′,5′-phosphorothioate, on the cAMP-dependent protein kinase-induced activity of

hepatic glycogen phosphorylase and glycogen synthase. *J. Biol. Chem.* **259,** 15294–15300 Medline

36. Bell, D., and McDermott, B. J. (1994) Use of the cyclic-AMP antagonist, Rp-cAMPS, to distinguish between cyclic-AMP-dependent and cyclic AMP-independent contractile responses in rat ventricular cardiomyocytes. *J. Mol. Cell. Cardiol.* **26,** 1439–1448 CrossRef Medline
37. Darszon, A., Sánchez-Cárdenas, C., Orta, G., Sánchez-Tusie, A. A., Beltrán, C., López-González, I., Granados-González, G., and Treviño, C. L. (2012) Are TRP channels involved in sperm development and function? *Cell Tissue Res.* **349,** 749–764 CrossRef Medline
38. Cohen, R., Buttke, D. E., Asano, A., Mukai, C., Nelson, J. L., Ren, D., Miller, R. J., Cohen-Kutner, M., Atlas, D., and Travis, A. J. (2014) Lipid modulation of calcium flux through CaV2.3 regulates acrosome exocytosis and fertilization. *Dev. Cell* **28,** 310–321 CrossRef Medline
39. Smith, J. F., Syritsyna, O., Fellous, M., Serres, C., Mannowetz, N., Kirichok, Y., and Lishko, P. V. (2013) Disruption of the principal, progesterone-activated sperm Ca^{2+} channel in a CatSper2-deficient infertile patient. *Proc. Natl. Acad. Sci. U.S.A.* **110,** 6823–6828 CrossRef Medline
40. Navarro, B., Miki, K., and Clapham, D. E. (2011) ATP-activated P2X2 current in mouse spermatozoa. *Proc. Natl. Acad. Sci. U.S.A.* **108,** 14342–14347 CrossRef Medline
41. Sun, X. H., Zhu, Y. Y., Wang, L., Liu, H. L., Ling, Y., Li, Z. L., and Sun, L. B. (2017) The Catsper channel and its roles in male fertility: A systematic review. *Reprod. Biol. Endocrinol.* **15,** 65 CrossRef Medline
42. Chung, J. J., Shim, S. H., Everley, R. A., Gygi, S. P., Zhuang, X. W., and Clapham, D. E. (2014) Structurally distinct Ca^{2+} signaling domains of sperm flagella orchestrate tyrosine phosphorylation and motility. *Cell* **157,** 808–822 CrossRef Medline
43. Navarrete, F. A., Alvau, A., Lee, H. C., Levin, L. R., Buck, J., Martin-De Leon, P., Santi, C. M., Krapf, D., Mager, J., Fissore, R. A., Salicioni, A. M., Darszon, A., and Visconti, P. E. (2016) Transient exposure to calcium ionophore enables *in vitro* fertilization in sterile mouse models. *Sci. Rep.* **6,** 33589 CrossRef Medline
44. Wiesner, B., Weiner, J., Middendorff, R., Hagen, V., Kaupp, U. B., and Weyand, I. (1998) Cyclic nucleotide-gated channels on the flagellum control Ca^{2+} entry into sperm. *J. Cell Biol.* **142,** 473–484 Medline
45. Kilic, F., Kashikar, N. D., Schmidt, R., Alvarez, L., Dai, L., Weyand, I., Wiesner, B., Goodwin, N., Hagen, V., and Kaupp, U. B. (2009) Caged progesterone: A new tool for studying rapid nongenomic actions of progesterone. *J. Am. Chem. Soc.* **131,** 4027–4030 CrossRef Medline
46. Weyand, I., Godde, M., Frings, S., Weiner, J., Müller, F., Altenhofen, W., Hatt, H., and Kaupp, U. B. (1994) Cloning and functional expression of a cyclic-nucleotide-gated channel from mammalian sperm. *Nature* **368,** 859–863 CrossRef Medline
47. Cisneros-Mejorado, A., and Sánchez Herrera, D. P. (2012) cGMP and cyclic nucleotide-gated channels participate in mouse sperm capacitation. *FEBS Lett.* **586,** 149–153 CrossRef Medline
48. Cisneros-Mejorado, A., Hernández-Soberanis, L., Islas-Carbajal, M. C., and Sánchez, D. (2014) Capacitation and Ca^{2+} influx in spermatozoa: Role of CNG channels and protein kinase G. *Andrology* **2,** 145–154 CrossRef Medline
49. Lishko, P. V., Botchkina, I. L., and Kirichok, Y. (2011) Progesterone activates the principal Ca^{2+} channel of human sperm. *Nature* **471,** 387–391 CrossRef Medline
50. Mannowetz, N., Miller, M. R., and Lishko, P. V. (2017) Regulation of the sperm calcium channel CatSper by endogenous steroids and plant triterpenoids. *Proc. Natl. Acad. Sci. U.S.A.* **114,** 5743–5748 CrossRef Medline
51. Xia, J., Reigada, D., Mitchell, C. H., and Ren, D. (2007) CATSPER channel-mediated Ca^{2+} entry into mouse sperm triggers a tail-to-head propagation. *Biol. Reprod.* **77,** 551–559 CrossRef Medline
52. Xia, J. S., and Ren, D. J. (2009) Egg coat proteins activate calcium entry into mouse sperm via CATSPER channels. *Biol. Reprod.* **80,** 1092–1098 CrossRef Medline